Gondwana Research 139 (2025) 136–146

Contents lists available at ScienceDirect

Gondwana Research

journal homepage: www.elsevier.com/locate/gr

Carbonate deposition in the Arctic during the Paleocene Eocene Thermal Maximum (PETM) and Early Eocene Climatic Optimum (EECO)

Henry W. Posamentier [a], Anatoly M. Nikishin [b,*], Ksenia F. Aleshina [b], Elizaveta A. Rodina [b], Alexander P. Afanasenkov [c], Steven L. Bachtel [d], Gillian R. Foulger [e]

[a] Posamentier Geosciences LLC, 2134 Sea Way, Bodega Bay, CA, USA
[b] Geological Faculty, Moscow State University, Moscow, Russia
[c] Rosgeo, Moscow, Russia
[d] AIMGeoanalytics, 101 S California Street, Missoula, MT 59801, USA
[e] Department of Earth Sciences, Durham University, Science Laboratories, South Rd. DH1 3LE, UK

A R T I C L E I N F O

Handling Editor: N. Rawlinson

Keywords:
Arctic
Carbonates
Paleocene Eocene Thermal Maximum
Early Eocene Climatic Optimum
Seismic stratigraphy
Mendeleev Rise

A B S T R A C T

Recently-acquired, high-quality seismic reflection profiles document the presence of possible carbonate deposits on the Mendeleev Rise in the Arctic Ocean during the Paleocene-Eocene Thermal Maximum and the Early Eocene Climatic Optimum. These deposits are concentrated at the crests of bathymetric highs and consist of clusters of buildups comprising small patch reefs overlain by larger, coalesced platforms, followed by back-stepped higher-relief platforms. The small buildups commonly are ~ 100–500 m in diameter and 50–100 m in height. The larger platforms are up to 3–7 km wide and up to 400 m thick. Some of the larger buildups are characterized by internal horizontally layered architecture, whereas others are characterized internally by clinoforms suggesting progradational growth. A common characteristic of these buildups is that they tend to achieve a common height (i.e., their tops align along the same level), typical of buildups sensitive to growth within the photic zone, whose upward growth is limited by sea level. The succession of buildup styles indicates carbonate factories under the influence of accelerating relative sea-level rise, which culminated in drowning and ultimate abandonment.

1. Introduction

Cenozoic shallow-water carbonates in the Arctic Ocean and Arctic islands and adjacent land have not been previously documented (e.g., Stein, 2019). However, the presence of deep-water mud-bearing biosiliceous ooze deposits has been documented by sampling of the Lomonosov Ridge (Moran et al., 2006; Brinkhuis et al., 2006; Backman et al., 2008) during the Arctic Coring Expedition (ACEX). The age of these deposits are Eocene (Ypresian), 50–45.4 Ma.

It is well known that the Arctic was likely ice free during the Paleocene Eocene Thermal Maximum (PETM) (Sluijs et al., 2006, 2008; Moran et al., 2006; Backman and Moran, 2009; Stein 2019), suggesting that these anomalously warm periods were characterized by annual temperatures that were in the order of 21°–22° C (Sluijs et al., 2006, 2008, 2009). Biostratigraphic evidence suggests the presence of temperate to subtropical flora on the fringing coastal and alluvial plains in Siberia, Canada, and Alaska during the late Paleocene and early Eocene (e.g., Akhmetiev, 2015; West et al., 2015; Suc et al., 2020; Bondarenko and Utescher, 2022; Blumenberg et al., 2024). This markedly warm period of time has been described as a “hothouse” or “greenhouse” time (Moran et al., 2006; Backman and Moran, 2009; Stein, 2019), though until the present study, there has been no evidence for widespread shallow-water carbonate deposition.

Plate reconstructions suggest that the Arctic Amerasia Basin was in a post-rift phase (Stein, 2019; Nikishin et al., 2021c) with somewhat restricted oceanic circulation during the Paleocene-Eocene (Stein, 2019). Likewise, plate reconstruction indicates that this area then as now was situated over the North Pole (O’Regan et al., 2008a; Scotese, 2014). Several bathymetric highs were present at that time, including the Lomonosov Ridge and the Mendeleev Rise (Nikishin et al., 2021b, 2021c) (Fig. 1). The present study will show that possible carbonate production created buildups of various sizes with diagnostic internal seismic character that has been recognized in other carbonate platforms globally. The platforms were especially active on the Mendeleev Rise paleo-bathymetric high.

The Mendeleev Rise is located within the Amerasia Basin between

* Corresponding author.
E-mail address: nikishin@geol.msu.ru (A.M. Nikishin).

https://doi.org/10.1016/j.gr.2024.11.011
Received 2 May 2024; Received in revised form 29 October 2024; Accepted 10 November 2024
Available online 9 December 2024
1342-937X/

the Podvodnikov-Makarov and Toll-Mendeleev-Nautilus deep-water basins (Fig. 1). Recent review of its structure was done by Nikishin et al. (2021a, 2021b, 2021c, 2023) where it was suggested that the Mendeleev Rise consisted of possible stretched continental crust terrane covered by basalts. The Mendeleev Rise is characterized by a relatively thickened crust up to 20–30 km comprising shallow-marine and continental volcanics with documented isotopic ages of 127–80 Ma (Coakley et al., 2016; Mukasa et al., 2020; Skolotnev et al., 2019, 2023; Nikishin et al., 2021b, 2021c, 2023) overlying a Paleozoic sedimentary cover (Skolotnev et al., 2019, 2023; Nikishin et al., 2021b, 2021c, 2023). Post-rift and post-volcanic regional subsidence started during the late Cretaceous and current water-depth is 1–2 km. Nikishin et al. (2023) presented an interpretation of seismic 2D data for the Alpha-Mendeleev Rise. They hypothesized that at least one buried high contained Eocene carbonates, a hypothesis that is considered in this paper using all available new seismic data (Nikishin et al., 2021a, 2023; Shimeld et al., 2021).

2. Data and methods

Recent geophysical surveys have yielded a regional grid of high-quality multi-channel seismic reflection data across the Arctic (Fig. 1) (Bruvoll et al., 2010; Weigelt et al., 2014; Coakley et al., 2016; Piskarev et al., 2019; Nikishin et al., 2021a, 2021b, 2021c, 2023; Shimeld et al., 2021). The dominant frequency of these data, 50–60 Hz, allowed for resolution of approximately 10 m (i.e., 1/4 seismic wavelength). Two versions of seismic streamer lengths were used. A 600 m long solid streamer was used when ice cover conditions existed or when an ice channel could close relatively quickly. A streamer 4500 m long and longer (solid or gel-filled) was used in the absence of solid ice cover and when an ice channel remained open for sufficient time for the survey. The streamer towage depth for most of the seismic acquisition was 15 m in order to keep it below any ice keels. The shotpoint spacing on most of the seismic lines was 50 m, with a record length of 12 s (Nikishin et el., 2021a). Seismic analyses of these data have formed the basis for a new comprehensive stratigraphic framework as well as plate reconstruction for the area (Brinkhuis et al., 2006; O'Regan et al., 2008b; Shephard et al., 2013; Weigelt et al., 2014; Nikishin et al., 2021a, 2021b, 2021c, 2023). Extensive coring and bottom sampling provided ground truth and calibration for these age models (Moran et al., 2006; Backman et al., 2008; Coakley et al., 2016; Homza and Bergman, 2019; Skolotnev et al., 2019; Nikishin, et al., 2021b, 2021c). Key data include results of the Integrated Ocean Drilling Program Expedition 302, Arctic Coring Expedition (ACEX) project (e.g. Moran et al., 2006; Backman et al., 2008) and deepwater geological expeditions in 2014 and 2016 (Mendeleev-2014 and Mendeleev-2016) using special submarine equipment to collect deepwater samples from outcrops (Skolotnev et al., 2019, 2023; Nikishin et al., 2021a). In addition, a few shallow stratigraphic boreholes were recently drilled by the Geologic Survey of Russia and oil company Rosneft in the Laptev, East-Siberian and Chukchi Seas with first results presented by Malyshev et al. (2024a, 2024b) and Petrov et al. (2023). Cenozoic to Jurassic strata were drilled and samples studied. Coal-bearing deposits were observed to be common within the Paleocene and Eocene sections.

Seismic stratigraphic analyses highlighted in the present study focused on evaluation of seismic reflection architecture and provide strong evidence for active shallow-water carbonate deposition over at least some of the paleo-bathymetric highs. The seismic stratigraphic approach taken was that outlined by Mitchum and Vail (1977) wherein 1) reflection terminations were identified and related to stratigraphic discontinuities, 2) the form and shape of individual seismic reflections were evaluated and related to stratigraphic architecture and ultimately to depositional elements, and 3) seismic reflection continuity and amplitude were evaluated as an indication of lithologies present. Depositional features that were identified were subsequently age-dated by relating them to the available stratigraphic framework.

3. Discussion

3.1. Regional stratigraphy

The stratigraphy of the Mendeleev Rise is based upon two data sets in

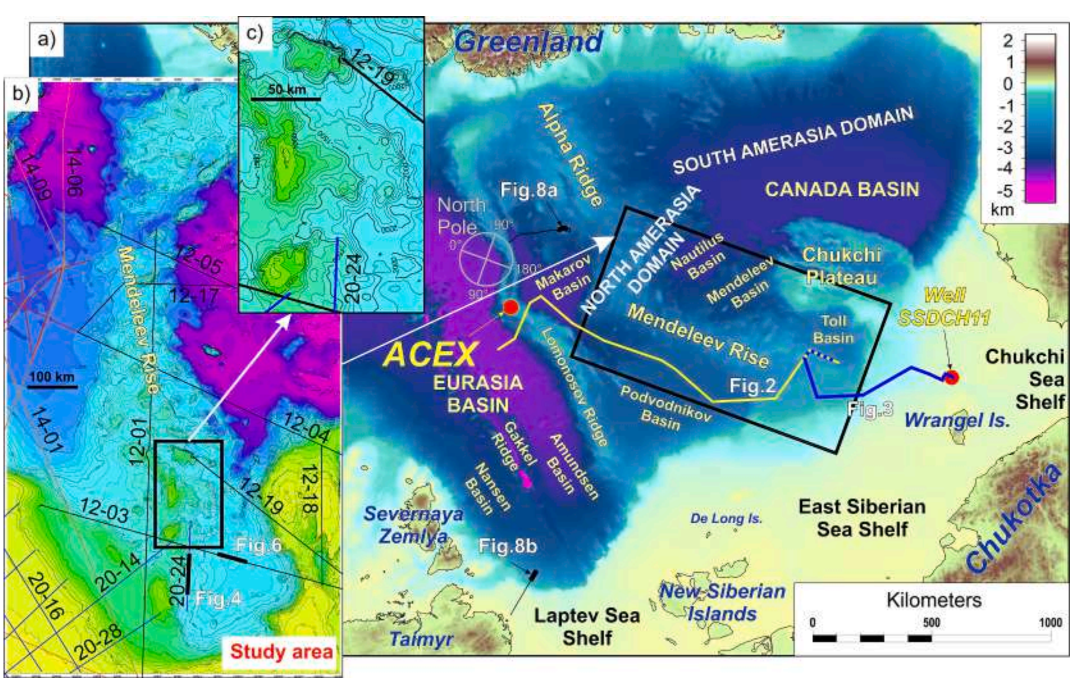

Fig. 1. a) Map showing key topographic elements of the arctic region (Jakobsson et al., 2020) as well as b) the location of key seismic lines within the study area (Nikishin et al., 2021a). Inset c) illustrates detailed bathymetry characterized by a rugose topography. Because the interpreted drowned carbonate buildups were subsequently overlain by isopachous deposits, the observed seafloor topography can serve as a proxy for PETM topography and therefore the morphology of interpreted carbonate platforms.

conjunction with the 2D seismic data: borehole data integrated with the regional seismic grid and sample collections using special underwater vehicles. Two regional seismostratigraphic units are recognized: HARS-1 and HARS-2 (Nikishin et al, 2021b). These units can be traced around main parts of the Eurasia and Amerasia basins (for details see Nikishin et al., 2021b). The level of interpreted carbonates in the Mendeleev Rise coincides with HARS-1 (56–45 Ma). The seismic section shown in Fig. 2 provides a tie between the ACEX well and the Mendeleev Rise and provides age calibration for the target section. This tie to available borehole data strongly suggests an age for the possible carbonate section close to 56–45 Ma. Another borehole that provides age data is the recently drilled well SSDCH-11 in the Chukchi Sea to the North-East of Wrangel Island (Malyshev et al., 2024b). That borehole penetrated an angular unconformity between Cenozoic and Lower Cretaceous deposits (Fig. 3b and e). Within the section correlative with the possible shallow-water carbonate deposits, early Paleocene and younger deposits were documented by microfossils (Malyshev et al., 2024a, 2024b).

Recently acquired sample collection using special underwater vehicles on the slopes of seamounts (Skolotnev et al., 2019, 2022, 2023; Nikishin et al., 2021a, 2023) provided further insights into the stratigraphy of the Mendeleev Rise. The Mendeleev Rise is characterized by Pre-Cenozoic horsts and half-grabens (Nikishin et al., 2023). As illustrated by Fig. 3b the upper part of the pre-Cenozoic structured section is characterized by high-amplitude seismic reflections that are interpreted as volcanics. Half-graben sections within this pre-Cenozoic section are wedge-shaped and similar in geometry to seaward-dipping reflectors (SDRs) of continental passive volcanic margins (Fig. 3b and d). Rock sampling has shown that the horsts are composed of sedimentary rocks of Paleozoic age, penetrated by intrusions (Skolotnev et al., 2023). Aptian-Albian sections containing volcanics (basalts, trachybasalts, trachyandesites) were identified on the horsts. U/Pb dating of igneous rocks showed that the typical age of the rocks is 114–110 Ma (the maximum age range is between 127 and 80 Ma) (Skolotnev et al., 2023). The first strata overlying the volcanics on the Mendeleev Rise are shallow-marine sandstones characterized by Barremian to Aptian fossils (Skolotnev et al., 2019, 2022; Nikishin et al., 2021a). Mukasa et al. (2020) obtained isotopic ages of basalts dredged from Chukchi Borderland northern slope characterized by ages close to 118–70 Ma. Isotopic data show that the interpreted carbonates lie between the Cretaceous volcanics and the sea floor, which currently lies at over 1500 m water depth. Consequently, a major flooding/drowning event, likely driven by tectonic subsidence, must have occurred between deposition of the shallow-water deposits immediately overlying the volcanic basement and the modern sea floor, which lies in deep water. Although subsidence associated would sediment compaction likely occurred as well, these effects would have been minimal compared with subsidence associated with regional tectonism.

3.2. Possible carbonates of the Mendeleev Rise

All regional seismic data were evaluated for the presence of possible carbonate buildups across the Mendeleev Rise. Because of the variable quality of the seismic data and the relatively sparse coverage, systematic mapping of potential buildups was not possible. However, we interpret numerous possible carbonate buildups based on one-line interpretations over several tectonic highs in the vicinity of the Mendeleev Rise (Figs. 3-6). The principal conclusion is that there are carbonate buildups across this structurally high setting and that they are of the same age (i.e., Eocene). Fig. 7 illustrates the map distribution of the observed possible buildups.

Features observed exclusively at the top of early Cenozoic paleobathymetric highs along the Mendeleev Rise reveal the presence of features (Fig. 3a and 4d) that are interpreted as shallow-water carbonate patch reefs and platforms very similar to Miocene platforms observed on seismic data in today's tropics and sub-tropics (Fig. 5) (Posamentier et al., 2010; Bashir et al., 2021; Makhankova et al., 2021). Two types of mounded features are observed: small conical-shaped mounded features approximately 100–500 m in diameter and 50–100 m in height, and larger massive mounds or platforms up to 3–7 km in diameter and up to 400 m in thickness. The smaller mounded features are observed to

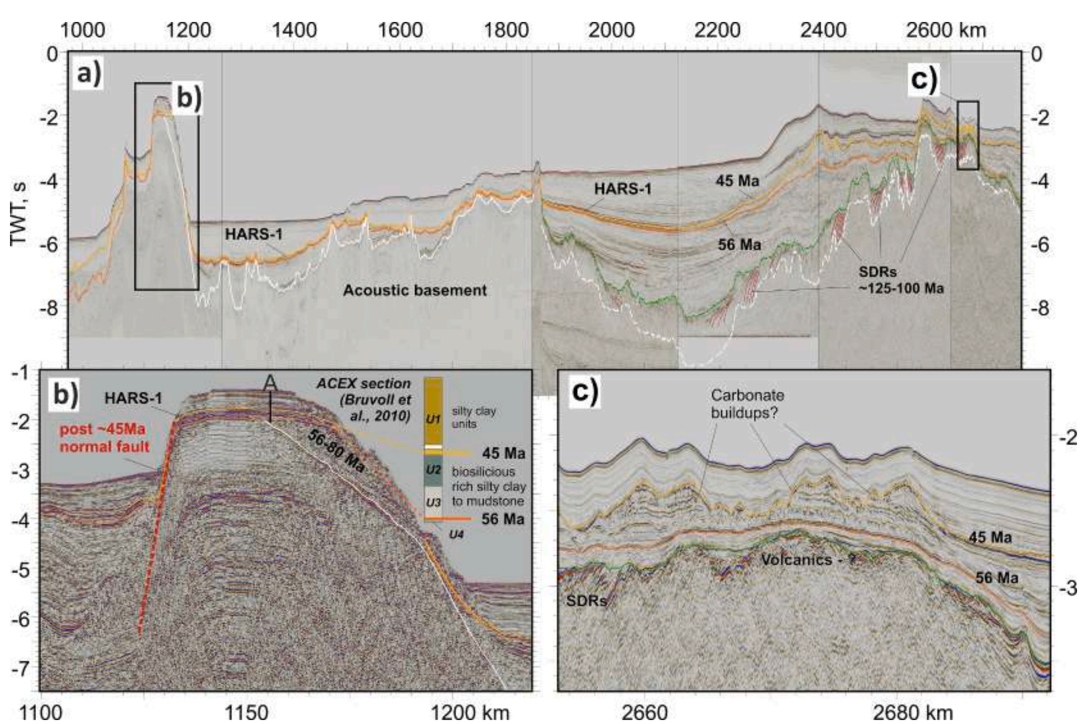

Fig. 2. a) Composite seismic profile from the acex borehole on the Lomonosov Ridge to the interpreted carbonates on the Mendeleev Rise (see Fig. 1 for location). Data from (Nikishin et al., 2021a; Nikishin et al., 2021b; Nikishin et al., 2023). b) – Detailed seismic section with ACEX borehole data, ACEX borehole data from (Bruvoll et al., 2010). c) – Detailed section illustrating interpreted carbonates. Seismic stratigraphic correlations suggest that the age of the interpreted shallow-water carbonates is between 56 Ma and 45 Ma.

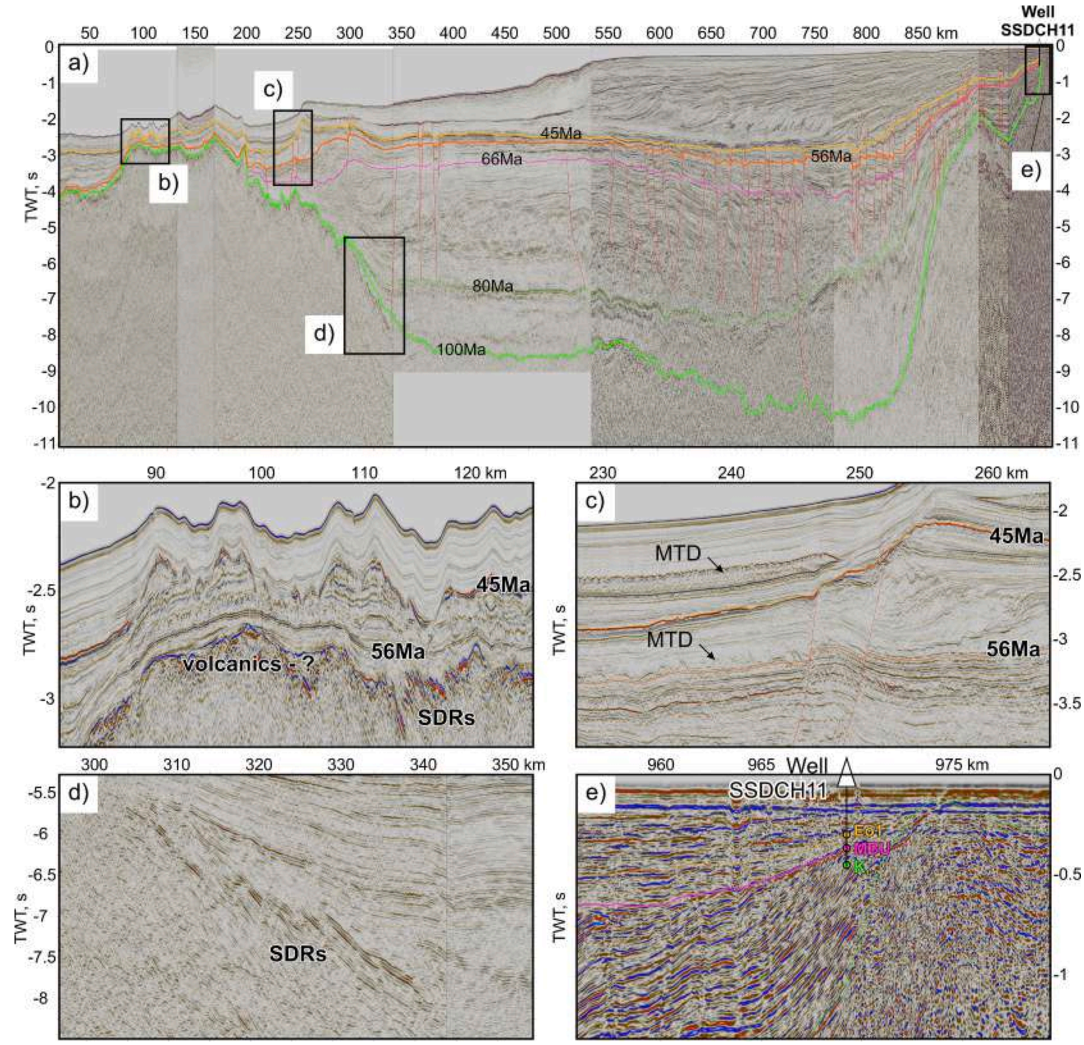

Fig. 3. a) Composite seismic profile from the chukchi sea borehole (SSDCH11) to carbonates on the Mendeleev Rise (seeFig. 1 for location). Data from (Nikishin et al., 2021a; Nikishin et al., 2021b; Nikishin et al., 2023; Malyshev et al., 2024b). Inset b) – detailed section illustrating interpreted carbonates; Inset c) – illustrating mass transport deposits (MTDs) suggesting the presence of a deep-water depositional environment; inset d) – possible SDRs with basalts (~125–100 Ma); inset e) – correlation with borehole SSDCH11 data. Seismic stratigraphic correlation supports the interpretation of an age between 56 Ma and 45 Ma.

overlie a continuous, essentially featureless (i.e., likely planar horizontal at the time of deposition) high-amplitude reflection and are widespread across the area of the paleo-bathymetric high. Internally, the larger interpreted buildups or platforms are characterized by internal horizontal reflections indicative of aggradational accretion of shallow-water carbonate deposits. Temporally, the small, mounded features are overlain by much larger mounded or platform features, which in places are conically-topped and in other places are flat-topped, and in places, characterized by internal horizontal reflections. Again, it is worth noting that these interpreted high-relief buildups lie directly above a package of planar parallel seismic reflections, which, in turn lie above likely volcanic basement, suggesting that these high-relief features significantly post-date basement structuring.

The overall succession represents a trend that has been observed in past studies (Posamentier et al., 2010): 1) platforms dominated by patch reefs, 2) coalescence of patch reefs into a large “mega-platforms”, 3) rapid aggradation (due to relative sea level rise) and eventual drowning. Their location directly above uplifted basement structural highs is consistent with the interpretation that these high-relief features, interpreted as carbonate buildups, nucleated on these bathymetric highs.

Although direct borehole calibration is not available at this time, we nonetheless interpret a carbonate origin for these features based upon observed seismic geometry and reflection character compared with analogs of known carbonate buildups that are strikingly similar, as well as based upon first principles regarding the stratigraphy of carbonate deposits (Burgess et al., 2013; Hendry et al., 2021). Fig. 5 illustrates a comparison between the features observed here and documented Miocene carbonate buildups from southeast Asia (compare Fig. 4c and 4d) (Posamentier et al., 2010). Despite the differences in local climate and age, the two features are virtually identical from a stratigraphic architectural perspective. In both instances we observe small cone-shaped features overlain by larger mounded platform stratigraphic architecture (Figs. 4 and 5). Internal to the larger platform facies, horizontal seismic reflections, and possible progradation can be observed (Figs. 4 and 6).

The scale of the observed features and the analog features is strikingly similar. In both instances, the buildups grade from small buildups at the base to overlying intermediate buildups to larger platform buildups at the top. The analog features, when mapped in 3D, are circular in outline and interpreted as small patch reefs (Fig. 5d and 5e). Unfortunately, without available 3D seismic data coverage, we cannot be certain of the map view of the features described here and can only infer their circular map pattern. The crests of these small, interpreted patch reefs as well as the larger platform buildups reach a common level, which is a characteristic common to shallow-water carbonate buildups. This common level is controlled by the depth of the photic zone

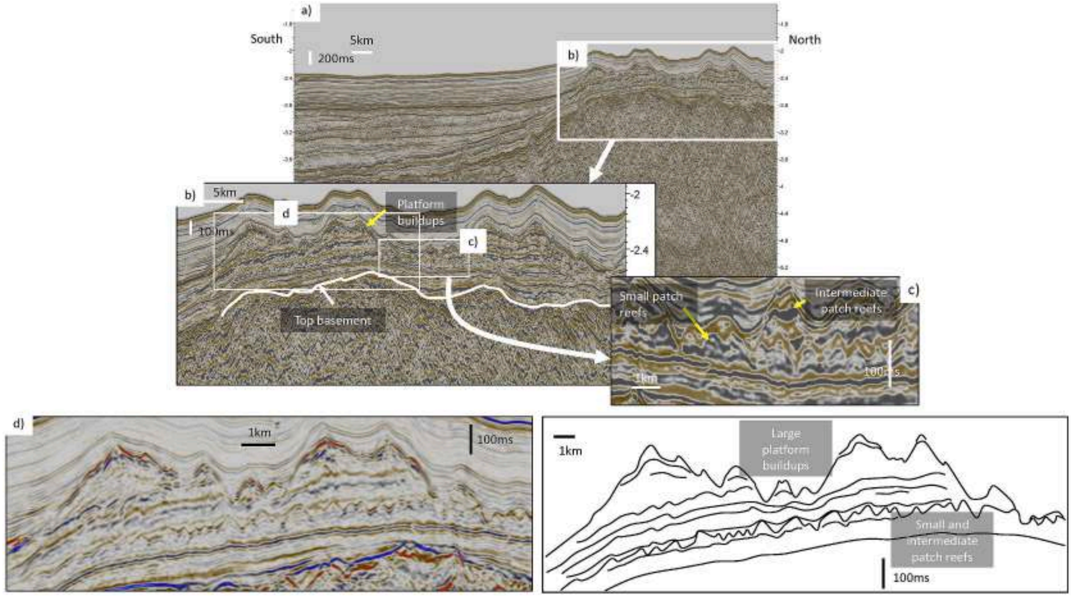

Fig. 4. a) Multi-channel seismic section (arc20-24) across the Mendeleev Rise (seeFig. 1 for location). b) Detail of interpreted carbonate buildups illustrating various size patch reefs and platforms. c and d) Detailed view of interpreted small and intermediate patch reefs characterized by small patch reefs at the base, culminating in larger platforms at the top, uninterpreted and interpreted.

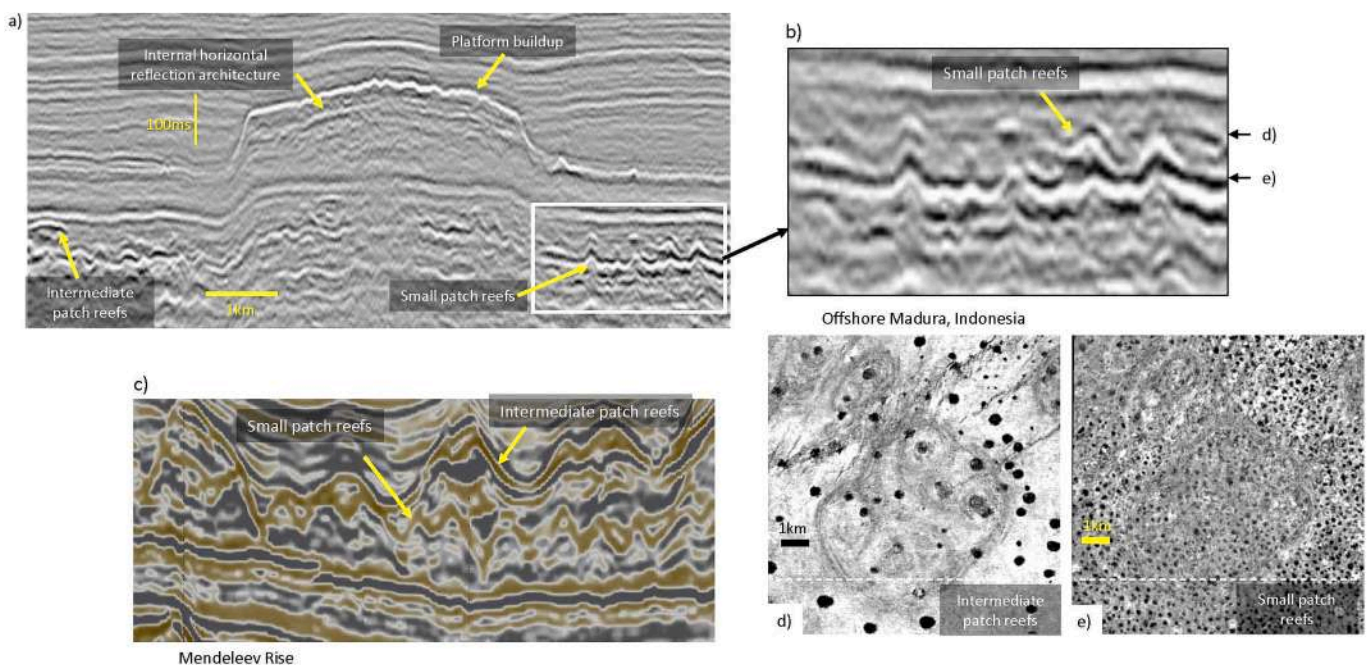

Fig. 5. Comparison between Miocene carbonate buildups (a, b, d, and e) from offshore Madura, Indonesia (Posamentier et al., 2010) and c) Mendeleev interpreted buildups (line location shown in Fig. 4). 3D seismic time slices (d and e) through small patch reefs shown in section view (a and b) with numerous small patch reefs (d) evolving into larger patch reefs (e) through time before culminating in significantly larger, higher-relief platforms (a).

comprising the upper layer of a body of water that receives sunlight. A modern analog that bears a striking resemblance to the Mendeleev Rise interpreted carbonate buildups is the Maldives islands. Here, too, a bathymetric basement high has allowed for the establishment of shallow-water carbonate buildups in the form of various sized patch reefs and platforms.

The section overlying the interpreted buildups is characterized by predominantly isopachous, continuous, moderate to high amplitude reflections that extend from over the Mendeleev Rise down the flanks on either side (Fig. 4b). This pattern is consistent with the process of pelagic and hemipelagic drape sedimentation that characterized this area subsequent to cessation of carbonate deposition, suggesting a drowning event related to accelerated tectonically-driven subsidence, which terminated carbonate production. Because of this drape style of deposition, the modern sea floor topography mirrors that of the PETM so that the irregularity of the modern sea-floor represents a proxy for the PETM paleotopography. Isolated platforms mapped in this way are up to 50 km wide (Fig. 1).

The greater thickness of the upper platform buildups relative to the smaller underlying interpreted patch reefs allows for internal

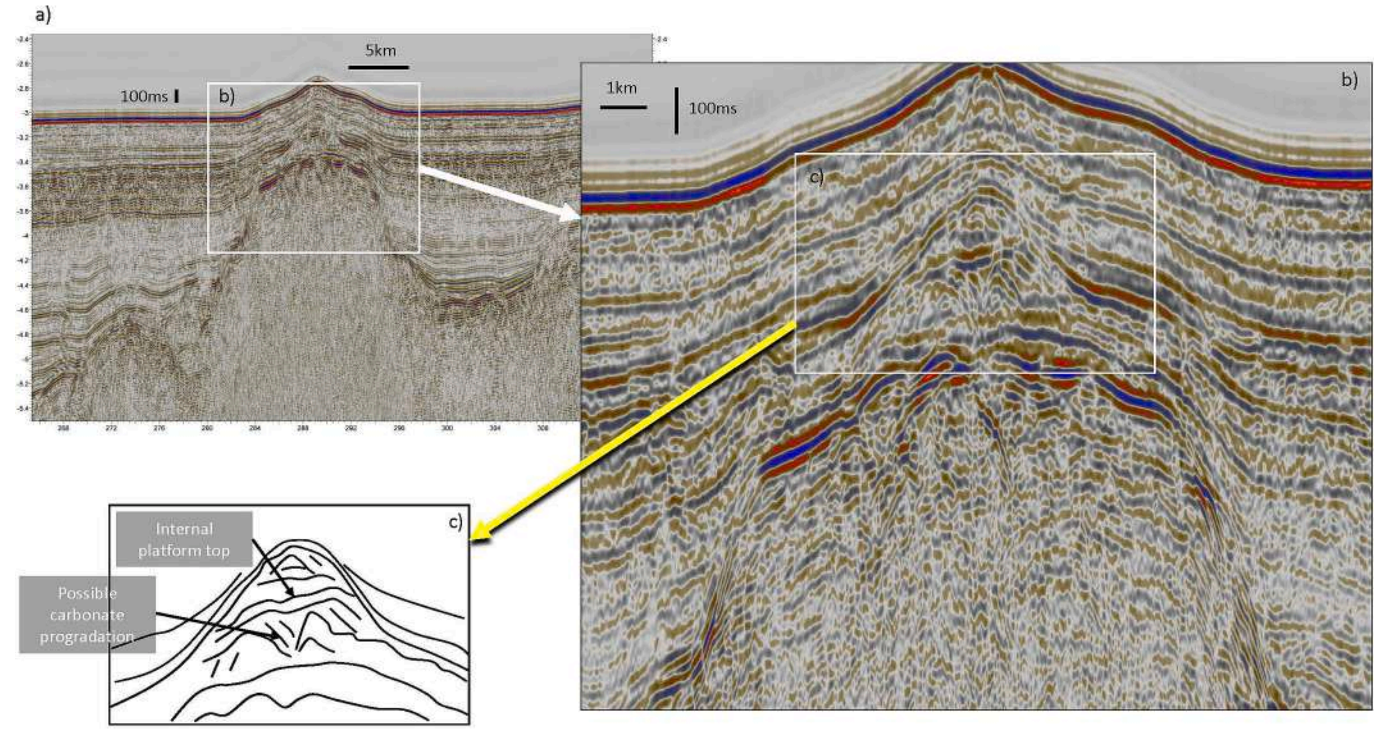

Fig. 6. a) seismic section (arc12-03) illustrating carbonate buildups from the Mendeleev Rise (seeFig. 1 for location). b) Detail of the seismic section highlighting the interpreted shallow-water carbonate deposits. c) Interpretation of the detailed seismic section focused on the shallow-water carbonates. Note the internal platform top inferred from the internal horizontal reflections.

architectural characteristics to be observed in these upper buildups. In places, possible horizontal reflections within the interpreted platforms can be observed (Figs. 4 and 6). Internal horizontal reflections are a characteristic typical of shallow-water carbonate platforms and indicate aggradation within the photic zone occurring in response to relative sea-level rise. This horizontal architecture or aggradational style of growth is a characteristic that differentiates carbonate buildups from volcanic edifices, which commonly are characterized by cone-in-cone rather than horizontally bedded internal stratigraphic architecture (Burgess et al., 2013; Posamentier et al., 2014; Hendry et al., 2021). Another differentiating characteristic of carbonate vs. volcanic edifices is that shallow-water carbonates tend to build simultaneously and top out at a common level (i.e., sea level is the controlling factor on carbonate buildup height), whereas volcanic edifice construction is not constrained vertically by sea level. Likewise, deep-water carbonates also would not have a common constraint to buildup height in that they grow well below sea level and commonly do not reach the photic zone. As Fig. 4 illustrates, especially for the many small patch reefs present towards the base of the interpreted carbonate complex, that these features are tightly clustered and reach approximately the same height. The presence of horizontal seismic reflections coupled with locally clinoforming progradational seismic reflections within the larger interpreted buildups further argues against these being of volcanic origin. The presence of continuous reflections of minimal relief just below the small, interpreted patch reefs as well as above is also consistent with an interpretation of a period of stasis prior and subsequent to initiation of carbonate production. Finally, the context of observing these features exclusively above paleobathymetric highs is consistent with a carbonate rather than a volcanic origin, inasmuch as volcanoes need not be local only to paleobathymetric highs.

The succession of smaller buildups followed by progressively larger, higher-relief buildups can be interpreted as carbonate sedimentation under the influence of accelerating relative sea-level rise that culminated in a drowning event, which resulted in total cessation of carbonate sedimentation. A similar stratigraphic succession of smaller buildups followed by progressively larger, higher-relief buildups offshore Madura, Indonesia, has been interpreted as being driven by accelerated relative sea-level rise (Fig. 5) (Posamentier et al., 2010). The drowning event within the study area in the region of the Mendeleev Rise likely occurred during the middle Eocene, coincident with accelerated tectonically driven subsidence that was associated with rapid subsidence of the North Chukchi Basin and major transgression in the order of 400–500 km (Nikishin et al., 2021b). This also was a time when climatic change towards cooler temperatures began.

3.3. Possible carbonate caps on eroded tops of Cretaceous and Paleocene volcanoes

Using seismic data, Funck and Shimeld (2023) described a submerged (i.e., with a top well below current sea level) seamount on the Alpha Ridge characterized by a truncated top and a size approximately 40x20 km (Fig. 8a). Samples containing hyaloclastics were collected from the seamount slope. The age of the volcanics is approximately 90 Ma (Funck and Shimeld, 2023). This volcaniclastic mound likely was eroded, possibly by subaerial processes, and was later flooded in response to accelerated subsidence before subsequently being buried by marine sediments. We propose that a carbonate platform developed during the transition from the possibly subaerial volcanic seamount to deep-marine seafloor (Fig. 8a). This possible carbonate platform lay above the late Cretaceous volcanics, consistent with an Eocene age that included the PETM and Early Eocene Climatic Optimum (EECO).

Nikishin et al. (2021b, 2021c) analyzed seismic data for the Laptev Sea Eurasia Basin continental margin and recognized a break-up unconformity with an age close to 56 Ma. A few possible magmatic features like intrusions and possible buried volcanos were described just below this unconformity suggesting that the age of magmatism is Paleocene or latest Cretaceous to Paleocene (Nikishin et al., 2021b). Several buried conical-type structures were discovered. (e.g., Fig. 8b). We suggest that here too, the presence of a Paleocene submarine massif characterized by erosional truncation at its top and subsequently overlain by deposits of

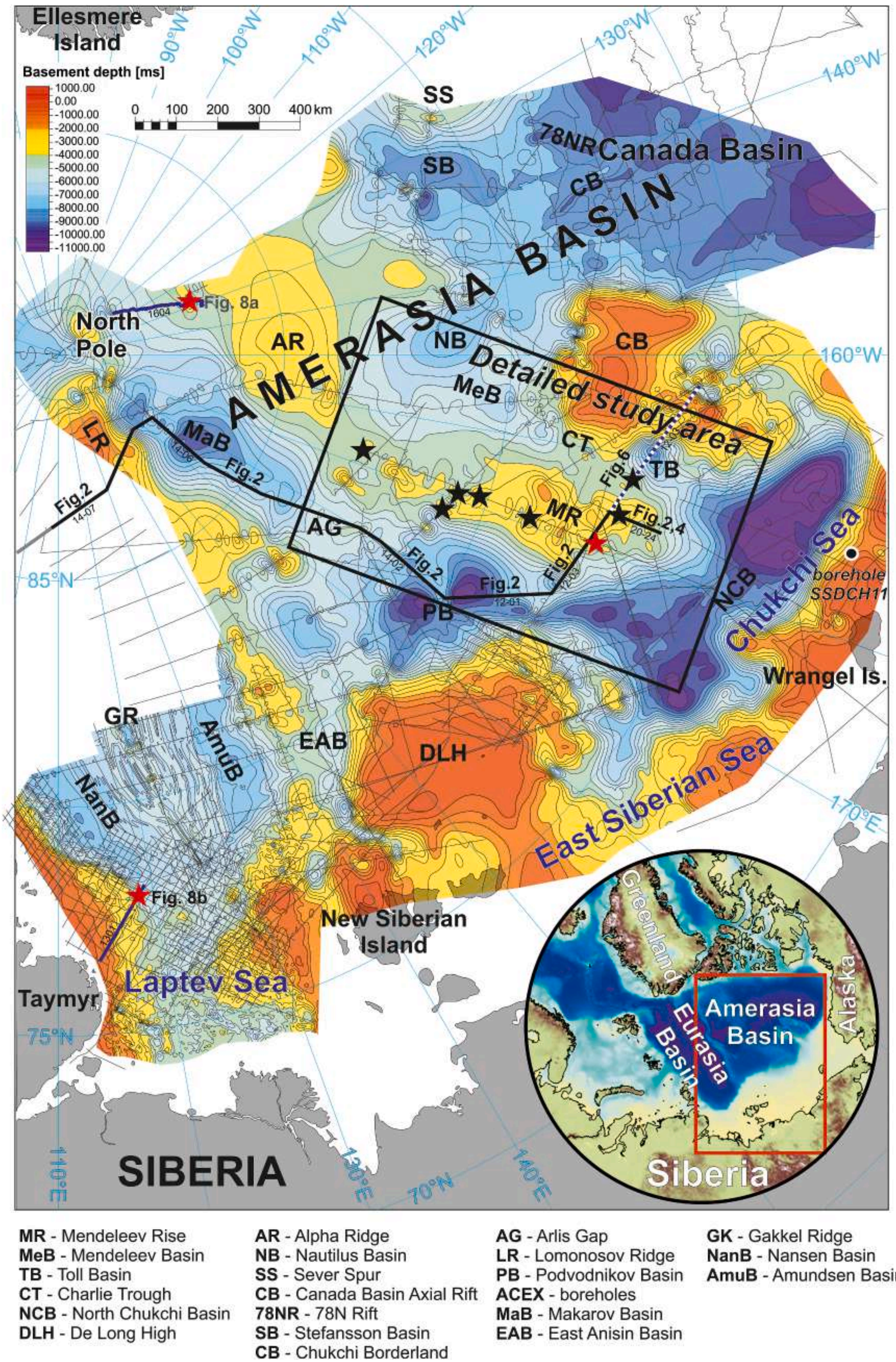

Fig. 7. Basement topography of the Mendeleev Rise region (modified after Nikishin et al., 2023, with new data added) and location of interpreted carbonate build-ups (stars). Black stars – interpreted carbonates on tectonic highs, red stars – interpreted carbonates on volcanic tops. (For interpretation of the references to colour in this figure legend, the reader is referred to the web version of this article.)

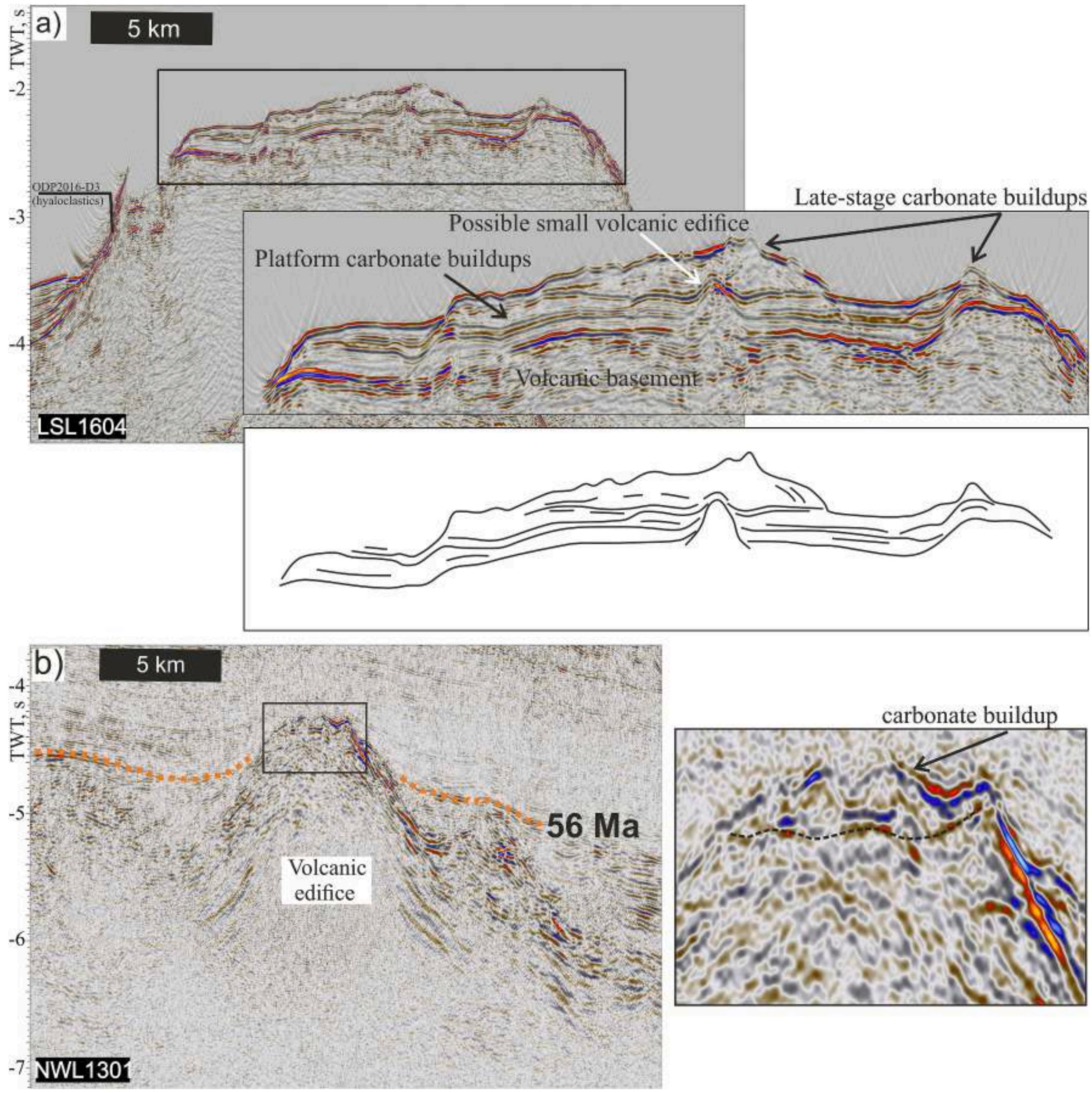

Fig. 8. a) Alpha ridge with Fedotov Cretaceous Volcano and carbonate cap. Seismic section from Funck and Shimeld (2023) with our interpretation of shallow-water carbonates. b) Laptev Sea continental slope and Paleocene volcano with possible carbonate cap (See Fig. 7 for location).

possible carbonates. The age of the carbonates was most likely post-Paleocene with an Eocene age that included PETM and EECO levels.

3.4. Why not volcanoes

Differentiating between carbonates and volcanics can be challenging and some examples of carbonates shown in this study may be equivocal. However, in those instances where the putative carbonates overlay horizontal reflections such as illustrated in Fig. 4d, a rejuvenated volcanic terrain overlying these horizontal reflections would not be a reasonable interpretation. Volcanic buildups subsequent to deposition of these horizontal reflections would have required the volcanics to have penetrated these reflections and re-established a volcanic terrain. Rather, we interpret the horizontal reflections as uniform (shallow?) marine sedimentation subsequently overlain by carbonate buildups (see discussion in section 3.2 above).

3.5. Comparison with carbonate buildups elsewhere

Numerous seismic stratigraphic units with a distinctive geometry suggestive of shallow-water carbonates have been observed on the Mendeleev Rise. Regional seismic and ACEX borehole-based studies from the nearby Lomonosov Ridge have recently shown that the section that is the focus of this study is approximately equivalent to the PETM and the EECO approximately 56–45 Ma (Sluijs et al., 2006, 2008; Backman and Moran, 2009; Shephard et al., 2013; Stein, 2019; Nikishin et al., 2021c). Largely based on Oxygen isotopes extracted from benthic foraminifera, temperatures were inferred to have been significantly higher than that of today. Annual temperatures up to 22° C with ice-free conditions have been suggested for the PETM. Faunal assemblages suggest “exceptionally warm and humid conditions” at that time (Stein, 2019; Salpin et al., 2019; Suc et al., 2020). Mollusk-derived stable isotopes from the Prince Creek Formation, Alaska, suggest annual shallow marine temperatures between 11°–22 °C (Brice et al., 1996; Singh et al., 2013). It is noteworthy that evidence of anomalously higher global temperatures at this time come from locations even far from the Arctic (Pollitt et al., 2012). Up until now, no evidence for active shallow-water carbonate deposition has been observed from any boreholes drilled in the Arctic. However, these boreholes were drilled primarily in locations where shallow-water carbonates would not have been deposited.

The presence of significant shallow-water carbonates in the Arctic that are strikingly similar to what is currently observed in warmer-water oceans, will have major significance to the greater scientific community. 1) it is the first time that the presence of a carbonate-friendly environment has been documented for the Arctic, with carbonate buildups – e.g., patch reefs and platforms – observed on paleo bathymetric highs, 2) the presence of these active carbonate factories on the Mendeleev Rise during the Paleocene/Eocene adds a significant data point to the discussion of climate change in general, 3) the presence of active shallow-water carbonate growth in a location that is characterized by periods of no daily sunlight for part of the year potentially opens up a new area of research regarding shallow-water carbonate growth in general, and 4) discovery of these examples of shallow-water carbonate growth highlights the need to better understand the paleo-tectonic and associated paleogeographic-driven oceanographic controls that allowed for a brief period of sufficiently warm water temperatures conducive to this growth (Fig. 9). Numerous studies focused on the stratigraphy of the Arctic address sea-level history with respect to regional tectonism (e.g., Moran et al., 2006; Backman et al., 2008; Hegewald and Jokat, 2013; Coakley et al., 2016; Homza and Bergman, 2019; Skolotnev et al., 2019; Nikishin, et al., 2021b, 2021c). Again, while it is known that the climate during this brief period of the PETM allowed for the development of temperate-type vegetation in the circum-Arctic environment, this paper presents the first documented examples for the presence of significant shallow-water carbonate development in this region. Discovery of possible Eocene shallow-water carbonates in the Arctic Ocean presents a challenge for Earth science. Because 2D seismic data is not sufficient to unequivocally confirm this interpretation, a borehole project to obtain samples from proposed carbonate bodies is required. Consequently, we propose a holistic international project to further study the Cenozoic climate history of the Arctic with special emphasis on confirming the presence of shallow-water carbonates.

Globally, carbonate structures during the PETM and EECO are well known (e.g., Perrin, 2002). They were primarily located in equatorial and tropical regions (Fig. 10). The dominant reef biota were algae, foraminifera, corals, bivalves, bryozoans, and worms (e.g., Perrin, 2002). In the current study area, rather than identify specifically which fauna were present, we can speculate that they may have included bryozoans, algae as well as other organisms. As expressed seismically, the carbonate structures of the Mendeleev Rise are similar to those of the Offshore Indus Basin in the Indian Ocean in terms of probable age and character of the geological structure (Shahzad et al., 2018; Shahzad et al., 2019). Likewise, the carbonate structures of the Mendeleev Rise are similar in their stratigraphic architecture to the well-studied late Oligocene-early Miocene carbonate platforms offshore Myanmar (Paumard et al., 2017; Teillet et al., 2020), as well as offshore Indonesia (Posamentier et al., 2010).

The depositional environment of the interpreted carbonate buildups is likely a shallow-water rather than deep-water setting. Deep-sea carbonates are well documented (e.g., Carvalho et al., 2023) and are observed at depths ranging from 250 m to over 1000 m. Because these buildups are not controlled by sea-level change, inasmuch as they lie well below the photic zone, they tend not nucleate at the top of bathymetric highs, nor do they build to a common level. In contrast, the carbonate buildups observed in this study clearly do nucleate over bathymetric highs, and do tend to build to a common height, thus suggesting a shallow-water, intra-photic zone environment here.

4. Conclusions

For the first time, shallow-water carbonate deposition in the Arctic during the PETM and the EECO has been documented based on seismic stratigraphic analyses of recently-acquired 2D seismic data. These deposits are observed on paleo-bathymetric highs associated with the Mendeleev Rise. Carbonate deposition evolves from small 100–500 m diameter patch reefs at the base, to larger 3–7 km wide platforms at the top. The stratigraphic architecture of these deposits is strikingly similar to analogous known shallow-water carbonate deposits elsewhere (Bachtel et al., 2004; Posamentier et al., 2010; Bashir et al., 2021; Makhankova et al., 2021). The carbonate deposits are interpreted to have evolved in response to accelerating relative sea-level rise (i.e., the combined effects of tectonically-driven subsidence and eustatic rise) that culminated in complete cessation of carbonate sedimentation during the early Eocene (Lutetian, 45 Ma), as this area ultimately became a deep-water environment, which currently lies at a depth of 1.5–2.0 km. The results presented here are preliminary and require ground truth in the form of borehole data for confirmation. To this end, we propose an international project to drill locations favorable for Arctic Cenozoic shallow-water carbonate bodies. Further focused research into Arctic depositional environments has the potential to change current models of the Cenozoic climatic history of this area.

Funding information

This study was supported by the Russian Science Foundation (Grant 24-17-00020).

CRediT authorship contribution statement

Henry W. Posamentier: Writing – review & editing, Writing – original draft, Conceptualization. **Anatoly M. Nikishin:** Writing – review & editing, Conceptualization. **Ksenia F. Aleshina:** Writing –

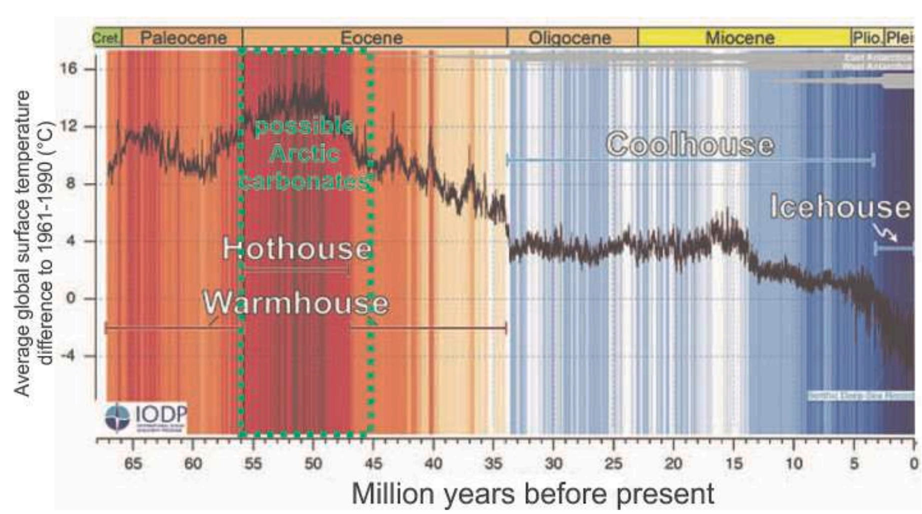

Fig. 9. Cenozoic paleoclimate (Westerhold et al., 2020; Planke et al., 2021) and interval of possible carbonate buildups.

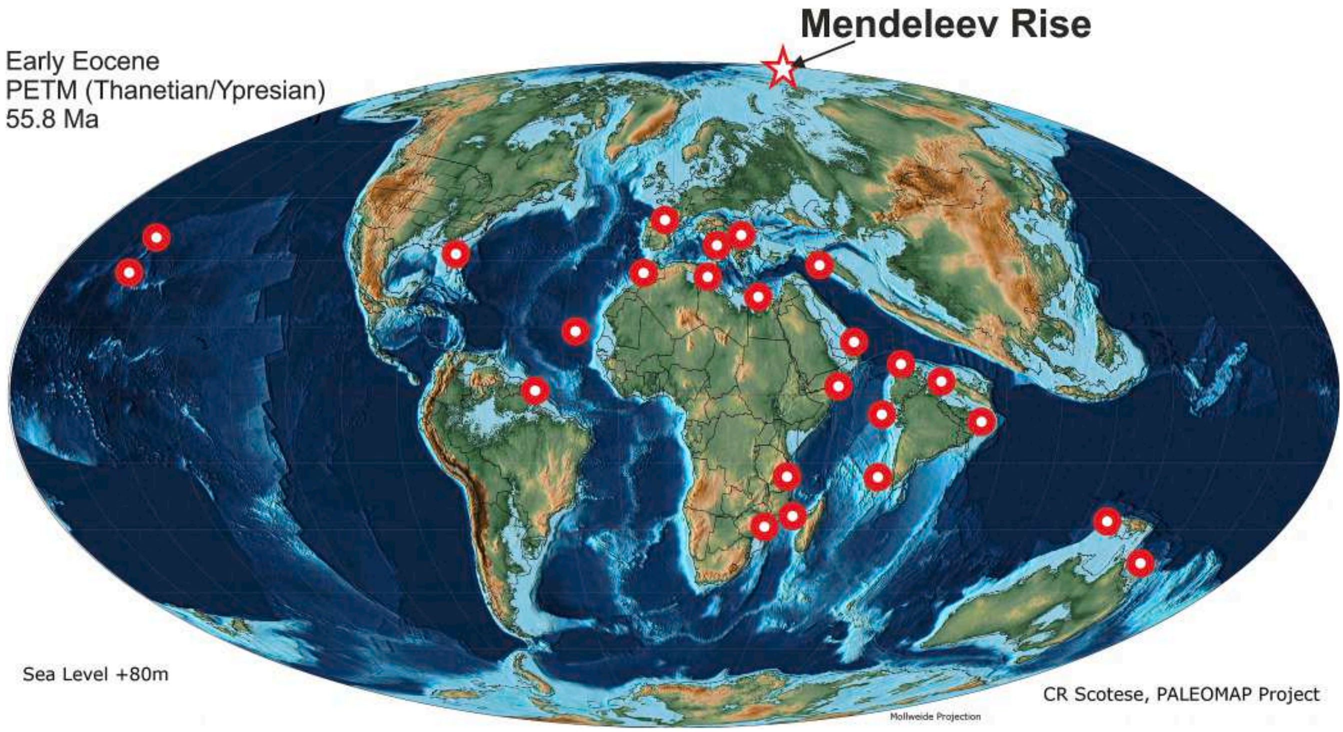

Fig. 10. Paleogeographic map for the PETM (Thanetian/Yprecian) time (Scotese, 2014) and global reef (carbonate build-ups) distribution (circles) corresponding to an interval characterized by sea level approximately 80 m higher than today. Mainly after Perrin (2002) and Shahzad et al. (2019). Star – location of possible Mendeleev Rise carbonates.

review & editing, Data curation. **Elizaveta A. Rodina:** Writing – review & editing, Investigation, Data curation. **Alexander P. Afanasenkov:** Writing – review & editing, Methodology, Data curation. **Steven L. Bachtel:** Methodology, Data curation. **Gillian R. Foulger:** Writing – review & editing, Data curation.

Declaration of competing interest

The authors declare that they have no known competing financial interests or personal relationships that could have appeared to influence the work reported in this paper.

Acknowledgements

The authors are grateful to the Ministry of Natural Resources and Environment of the Russian Federation, and to the Federal Subsoil Resources Management Agency (Rosnedra) for the opportunity to publish this paper. We thank N. Rawlinson and W. Geissler for constructive reviews of the paper.

References

Akhmetiev, M.A., 2015. High-latitude regions of Siberia and Northeast Russia in the Paleogene: Stratigraphy, flora, climate, coal accumulation. Stratigr. Geol. Correl. 23 (4), 421–435.

Bachtel., S.L., Dunn, P.A., Rahardjanto, S.P., Kissling R.D., Martono, D., and Macdonald, B.A., 2004. Seismic stratigraphic evolution of the Miocene-Pliocene Segitiga Platform, East Natuna Sea, Indonesia: The origin, growth, and demise of an isolated carbonate platform. In: Eberli, G.P., Masaferro, J.L., and Sarg, J.F.R., eds., Seismic imaging of carbonate reservoirs and systems. AAPG Memoir 81, p. 309-328.

Backman, J., Moran, K., 2009. Expanding the Cenozoic paleoceanographic record in the central Arctic Ocean: IODP Expedition 302 synthesis. Central Eur. J. Geosci. 1, 157–175.

Backman, J., Jakobsson, M., Frank, M., Sangiorgi, F., Brinkhuis, H., Stickley, C., et al., 2008. Age model and core-seismic integration for the Cenozoic Arctic coring expedition sediments from the Lomonosov Ridge. Paleoceanography 23, 1851–1894.

Bashir, Y., Faisal, M.A., Biswas, A., Babasafari, A.A., Ali, S.H., Imran, Q.S., Siddiqui, N.A., Ehsan, M., 2021. Seismic expression of Miocene carbonate platform and reservoir characterization through geophysical approach: application in central Luconia, offshore Malaysia. J. Petroleum Exploration and Production 11, 1533–1544.

Blumenberg, M., Naafs, B.D., Luckge, A., Lauretano, V., Schefuss, E., Galloway, G., Scheeder, G., Reinhardt, L., 2024. Biomarker reconstruction of a high-latitude late Paleocene to early Eocene coal swamp environment across the PETM and ETM-2 (Ellesmere Island, Arctic Canada). Paleoceanogr. Paleoclimatol. 39, e2023PA004712. https://doi.org/10.1029/2023PA004712.

Bondarenko, O.V., Utescher, T., 2022. Late early to early middle Eocene climate and vegetation change at Tastakh Lake (northern Yakutia, eastern Siberia). Palaeobiodiversity and Palaeoenvironments. https://doi.org/10.1007/s12549-022-00530-6.

Brice, K.L., Arthur, M.A., Marincovich Jr., L., 1996. Late Paleocene Arctic Ocean shallow-marine temperatures from mollusk stable isotopes. Paleoceanography 11, 241–249.

Brinkhuis, H., Schouten, S., Collinson, M.E., Sluijs, A., Damsté, J.S.S., Dickens, G.R., et al., 2006. Episodic fresh surface waters in the Eocene Arctic Ocean. Nature 441, 606–609.

Bruvoll, V., Kristoffersen, Y., Coakley, B.J., Hopper, J.R., 2010. Hemipelagic deposits on the Mendeleev and northwestern Alpha submarine ridges in the Arctic Ocean: acoustic stratigraphy, depositional environment and an inter-ridge correlation calibrated by the ACEX results. Mar. Geophys. Res. 31, 149–171. https://doi.org/10.1007/s11001-010-9094-9.

Burgess, P.M., Winefield, P., Minzoni, M., Elders, C., 2013. Methods for identification of isolated carbonate buildups from seismic reflection data. AAPG Bull. 97, 1071–1098.

Carvalho, N.F., Waters, L.G., Arantes, R.C.M., Couto, D.M., Cavalcanti, G.H., Güth, A.Z., Falcão, A.P.C., Nagata, P.D., Hercos, C.M., Sasaki, D.K., Dottori, M., Cordes, E.E., and Sumida, P.Y.G., 2023. Underwater surveys reveal deep-sea corals in newly explored regions of the southwest Atlantic. Commun. Earth Environ. 4, 282 (2023). doi: 10.1038/s43247-023-00924-0.

Coakley, B., Brumley, K., Lebedeva-Ivanova, N., Mosher, D., 2016. Exploring the geology of the central Arctic Ocean; understanding the basin features in place and time. J. Geol. Soc. London. 173, 967–987. https://doi.org/10.1144/jgs2016-082.

Funck, T., Shimeld, J., 2023. Crustal structure and magmatism of the Marvin Spur and northern Alpha Ridge, Arctic Ocean. Geophys. J. Int. 233 (1), 740–768. https://doi.org/10.1093/gji/ggac480.

Hegewald, A., Jokat, W., 2013. Tectonic and sedimentary structures in the northern Chukchi region, Arctic Ocean. J. Geophys. Res. 118, 3285–3296. https://doi.org/10.1002/jgrb.50282.

Hendry, J., Burgess, P., Hunt, D., Janson, X., and Zampetti, V., 2021. Seismic characterization of carbonate platforms and reservoirs: an introduction and review, In: Hendry, J., Burgess, P., Janson, X., and Zampetti, V., eds. Seismic Characterization of Carbonate Platforms and Reservoirs. Geological Society, London, Special Publication 509, 1-28.

Homza, T.X., Bergman, S.C., 2019. A geologic interpretation of the Chukchi Sea Petroleum Province: Offshore Alaska. AAPG Mem. 119. https://doi.org/10.1306/AAPG119.

Jakobsson, M., Mayer, L.A., Bringensparr, C., et al., 2020. The International Bathymetric Chart of the Arctic Ocean Version 4.0. *Sci Data* 7, 176. https://doi.org/10.1038/s41597-020-0520-9.
Makhankova, A., Sautter, B., Mathew, M., Menier, D., Poppelreiter, M., 2021. Seismic stratigraphy and sedimentology of a Miocene carbonate platform in Luconia, South China Sea. Geol. J. 56, 1–17.
Malyshev, N.A., Verzhbitsky, V.E., Danilkin, S.M., Kolyubakin, A.A., Ershova, V.B., Borodulin, A.A., Obmetko, V.V., Komissarov, D.K., Pashali, A.A., Boldyrev, M.L., Vasilyeva, I.S., Rogov, M.A., Popova, A.B., Vasilyev, V.E., Novikov, S.S., Gatovsky, Y. A., Aleksandrova, G.A., Lidskaya, A.V., Simakova, A.N., Lopatina, D.A., Bordunov, S. I., Stupakova, A.V., Suslova, A.A., Nikishin, A.M., Lakeev, V.G., Lukashev, R.V., 2024a. Stratigraphic Drilling in the Northeastern Part of Laptev Sea: First Results. Doklady Earth Sciences Vol. 515, Part 1, 563–572. https://doi.org/10.1134/S1028334X23603310.
Malyshev, N.A., Verzhbitsky, V.E., Kolyubakin, A.A., Komissarov, D.K., Borodulin, A.A., Obmetko, V.V., Boldyrev, M.L., Popova, A.B., Danilkin, S.M., Vasilyeva, I.S., Timoshenko, T.A., Stavitskaya, V.N., Novikov, S.S., Shein, V.A., Vasilyev, V.E., Alexandrova, G.N., Gatovsky, Y.A., Suslova, A.A., Stupakova, A.V., Nikishin, A.M., Lakeev, V.G., Lukashev, R.V., 2024b. Technological aspects and experience of stratigraphic drilling in the seas of the Russian Arctic. Geologiya Nefti i Gaza, N 3, 19–30. https://doi.org/10.47148/0016-7894-2024-3-19-30. In Russ.
Mitchum R.M., Jr., and Vail, P.R., 1977. Seismic stratigraphy and global changes of sea level, Part seven: seismic stratigraphic interpretation procedure. In: Payton, C.E. ed., Seismic Stratigraphy — Applications to Hydrocarbon Exploration. AAPG Mem. 26, 135-144.
Moran, K., Backman, J., Brinkhuis, H., Clemens, S.C., Cronin, T., Dickens, G.R., et al., 2006. The Cenozoic palaeoenvironment of the Arctic Ocean. Nature 441, 601–605. https://doi.org/10.1038/nature04800.
Mukasa, S.B., Andronikov, A., Brumley, K., Mayer, L.A., Armstrong, A., 2020. Basalts from the Chukchi Borderland: 40Ar/39Ar Ages and Geochemistry of submarine intraplate lavas dredged from the western Arctic Ocean. Am. Geophys. Union 125. https://doi.org/10.1029/2019JB017604.
Nikishin, A.M., Petrov, E.I., Cloetingh, S., Korniychuk, A.V., Morozov, A.F., Petrov, O.V., Poselov, V.A., Beziazykov, A.V., Skolotnev, S.G., Malyshev, N.A., Verzhbitsky, V.E., Posamentier, H.W., Freiman, S.I., Rodina, E.A., Startseva, K.F., Zhukov, N.N., 2021a. Arctic Ocean Mega Project: Paper 1 - Data collection. Earth-Sci. Rev. 217, 103559. https://doi.org/10.1016/j.earscirev.2021.103559.
Nikishin, A.V., Petrov, E.I., Cloetingh, S., Freiman, S.I., Malyshev, N.A., Morozov, A.F., Posamentier, H.W., Verzhbitsky, V.E., Zhukov, N.N., Startseva, K.F., Rodina, E.A., 2021b. Arctic Ocean Mega Project: Paper 2 – Arctic stratigraphy and regional tectonic structure. Earth Sci. Rev. 217, 103581. https://doi.org/10.1016/j.earscirev.2021.103581.
Nikishin, A.V., Petrov, E.I., Cloetingh, S., Freiman, S.I., Malyshev, N.A., Morozov, A.F., Posamentier, H.W., Verzhbitsky, V.E., Zhukov, N.N., Startseva, K.F., 2021c. Arctic Ocean Mega Project: Paper 3 – Mesozoic to Cenozoic geological evolution. Earth Sci. Rev. 217, 103034. https://doi.org/10.1016/j.earscirev.2019.103034.
Nikishin, A.M., Rodina, E.A., Startseva, K.F., Foulger, G.R., Posamentier, H.W., Afanasenkov, A.P., Chernykh, A.A., Malyshev, N.A., Petrov, E.I., Skolotnev, S.G., Verzhbitsky, V.E., Yakovenko, I.V., 2023. Alpha-Mendeleev Rise, Arctic Ocean: A double volcanic passive margin. Gondwana Res. https://doi.org/10.1016/j.gr.2022.10.010.
O'Regan, M., Moran, K., Backman, J., Jakobsson, M., Sangiorgi, F., Brinkhuis, H., Pockalny, R., Skelton, A., Stickley, C., Koç, N., Brumsack, H.-J., Willard, D., 2008. Mid Cenozoic tectonic and paleoenvironmental setting of the central Arctic Ocean. Paleoceanography 23, PA1S20. https://doi.org/10.1029/2007PA001559.
O'Regan, M., King, J., Backman, J., Jakobsson, M., Pälike, H., Moran, K., et al., 2008b. Constraints on the Pleistocene chronology of sediments from the Lomonosov Ridge. Paleoceanography 23, PA1S19 (2008b).
Paumard, V., Zuckmeyer, E., Boichard, R., Jorry, S.J., Bourget, J., Borgomano, J., Maurin, T., Ferry, J.-N., 2017. Evolution of Late Oligocene - Early Miocene attached and isolated carbonate platforms in a volcanic ridge context (Maldives type), Yadana field, offshore Myanmar. Mar. Pet. Geol. 81, 361–387. https://doi.org/10.1016/j.marpetgeo.2016.12.012.
Perrin, C., 2002, Tertiary: the emergence of modern reef ecosystems. In: Phanerozoic Reef Patterns. SEPM (Society for Sedimentary Geology), Tulsa, Okla., U.S.A, pp. 587–618.
Petrov, O.V., Nikishin, A.M., Petrov, E.I., Tatarinov, V.Y., Kashubin, S.N., Prishchepenko, D.V., Malyshev, N.A., Danilkin, S.M., Verzhbitsky, V.E., Kolyubakin, A.A., Komissarov, D.K., Stavitskaya, V.N., Shurekova, O.V., Razumkova, E.S., Tolmacheva, T.Y., Leontiev, D.I., Tokarev, M.Y., Ponimaskin, A.I., Zamotina, Z.S., 2023. First Results of Stratigraphic Drilling in the East Siberian Sea Focused on Geological Studies of the Suture Zone of the Continental Shelf's Marginal Structures and Deep-Water Areas of the Arctic Ocean. Doklady Earth Sci. Vol. 512 Part 2, 1014–1023. https://doi.org/10.1134/S1028334X23601256.
Piskarev, A., Poselov, V., and Kaminsky, V., eds., 2019. Geologic structures of the Arctic Basin (Springer International Publishing,). doi: 10.1007/978-3-319-77742-9.
Planke, S., Berndt, C., Alvarez Zarikian, C.A., 2021. Expedition 396 Scientific Prospectus: Mid-Norwegian Continental Margin Magmatism. International Ocean Discovery Program. https://doi.org/10.14379/iodp.sp.396.2021.
Pollitt, D.A., Anthonissen, E., Saller, A.H., BouDagher-Fadel, M.K., Dickson, J.A.D., 2012. Abrupt early Eocene global climatic change as a control of carbonate facies and diagenesis: a new record of the Paleocene-Eocene Thermal Maximum in the Umm er Radhuma Formation, Saudi Arabia and Kuwait. Terra Nova 24, 487–498. https://doi.org/10.1111/j.1365-3121.2012. 01087.x.
Posamentier, H.W., Laurin, P., Warmath, A., Purnama, M., and Drajat, D., 2010. Seismic Stratigraphy and Geomorphology of Oligocene to Miocene Carbonate Buildups, Offshore Madura, Indonesia. In: Morgan, W.A., George, A.D., Harris, P.M., Kupecz, J. A., and Sarg, J.F. Cenozoic Carbonate Systems of Australasia. SEPM Special Publication 95, 104-121.
Posamentier, H.W., Aydemir, V., Sipahioglu, Ö, Korucu, Ö., Roe, S., Abriel, W., Nantais, P., and Welch, R., 2014. Volcanic deposits in the Black Sea – seismic recognition criteria for differentiating volcanics from carbonates. AAPG Annual Conference, Houston TX, April 6-9, 1014.
Salpin, M., Schnyder, J., Baudin, F., Suan, G., Suc, J.-P., Popescu, S.-P., Fauquette, S., Reinhardt, L., Schmitz, M.D., and Labrousse. L., 2019. Evidence for subtropical warmth in the Canadian Arctic (Beaufort-Mackenzie, Northwest Territories, Canada) during the early Eocene. In: Piepjohn, K., Strauss, J.V., Reinhardt, L., and McClelland, W.C., eds., Circum-Arctic Structural Events: Tectonic Evolution of the Arctic Margins and Trans-Arctic Links with Adjacent Orogens. Geol. Soc. of Am. Special Paper 541. doi: 10.1130/2018.2541(27).
Scotese, C.R., 2014. Atlas of Paleogene Paleogeographic Maps (Mollweide Projection), Maps 8-15, Volume 1, The Cenozoic, PALEOMAP Atlas for ArcGIS, PALEOMAP Project, Evanston, IL. Technical Report. doi:10.13140/2.1.3417.6961.
Shahzad, K., Betzler, C., Ahmed, N., Qayyum, F., Spezzaferri, S., Qadir, A., 2018. Growth and demise of a Paleogene isolated carbonate platform of the Offshore Indus Basin, Pakistan: effects of regional and local controlling factors. Int. J. Earth Sci. (Geol Rundsch) 107, 481–504. https://doi.org/10.1007/s00531-017-1504-7.
Shahzad, K., Betzler, C., Qayyum, F., 2019. Controls on the Paleogene carbonate platform growth under greenhouse climate conditions (Offshore Indus Basin). Mar. Pet. Geol. 101, 519–539. https://doi.org/10.1016/j.marpetgeo.2018.12.025.
Shephard, G.E., Müller, R.D., Seton, M., 2013. The tectonic evolution of the Arctic since Pangea breakup: Integrating constraints from surface geology and geophysics with mantle structure. Earth Sci. Rev. 124, 148–183.
Shimeld, J., Boggild, K., Mosher, D.C., and Jackson, H.R., 2021. Reprocessed multi-channel seismic-reflection data set from the Arctic Ocean, collected using icebreakers between 2007-2011 and 2014-2016 for the Canadian Extended Continental Shelf program. Geological Survey of Canada, Open File 8850, 1 .zip file. doi: 10.4095/329248.
Singh, R.K., Maheshwari, M., Oza, S.R., Kumar, R., 2013. Long-term variability in Arctic Sea surface temperatures. Polar Sci. 7, 233–240.
Skolotnev, S., Aleksandrova, G., Isakova, T., Tolmacheva, T., Kurilenko, A., Raevskaya, E., Rozhnov, S., Petrov, E., Korniychuk, A., 2019. Fossils from seabed bedrocks: Implications for the nature of the acoustic basement of the Mendeleev Rise (Arctic Ocean). Mar. Geol. 407, 148–163. https://doi.org/10.1016/j.margeo.2018.11.002.
Skolotnev, S.G., Freiman, S.I., Khisamutdinova, A.I., Ermolaev, B.V., Okina, O.I., Skolotneva, T.S., 2022. Sedimentary rocks in the basement of the alpha–mendeleev rise, Arctic Ocean. Lithology and Mineral Resources 57 (2), 121–142. https://doi.org/10.1134/S0024490222020079.
Skolotnev, S.G., Fedonkin, M.A., Korniychuk, A.V., 2023. New data on the age of magmatic rocks of the Alpha-Mendeleev Rise (Arctic Ocean): results of isotopic U/Pb dating of zircons. Dokl. Earth Sci. https://doi.org/10.1134/S1028334X23601736.
Sluijs, A., Schouten, S., Pagani, M., Woltering, M., Brinkhuis, H., Damsté, J.S.S., the Expedition 302 Scientists, 2006. Subtropical Arctic Ocean temperatures during the Palaeocene/Eocene thermal maximum. Nature 441, 610–613.
Sluijs, A., Röhl, U., Schouten, S., Brumsack, H.J., Sangiorgi, F., Sinninghe Damsté, J.S., Brinkhuis, H., 2008. Arctic late Paleocene–early Eocene paleoenvironments with special emphasis on the Paleocene-Eocene Thermal Maximum (Lomonosov Ridge, Integrated Ocean Drilling Program Expedition 302). Paleoceanography 23, PA1S11.
Sluijs, A., Schouten, S., Donders, T.H., Schoon, P.L., Röhl, U., Reichart, G.J., et al., 2009. Warm and wet conditions in the Arctic region during Eocene Thermal Maximum 2. Nat. Geosci. 2, 777–780.
Stein, R., 2019. The Late Mesozoic-Cenozoic Arctic Ocean climate and sea ice history: a challenge for past and future scientific ocean drilling. Paleoceanogr. Paleoclimatol. 34, 1851–1894. https://doi.org/10.1029/2018PA003433.
Suc, J.-P., Fauquette, S., Popescu, S.-M., Robin, C., 2020. Subtropical mangrove and evergreen forest reveal Paleogene terrestrial climate and physiography at the North Pole. Palaeogeography, Palaeoclimatology, Palaeoecology 551, 109755. https://doi.org/10.1016/j.palaeo.2020.109755.
Teillet, T., Fournier, F., Montaggioni, L.F., BouDagher-Fadel, M., Borgomano, J., Braga, J.C., Villeneuve, Q., Hong, F., 2020. Development patterns of an isolated oligo-mesophotic carbonate buildup, early Miocene, Yadana field, offshore Myanmar. Marine and Petroleum Geology 111, 440–460. https://doi.org/10.1016/j.marpetgeo.2019.08.039.
Weigelt, E., Jokat, W., Franke, D., 2014. Seismostratigraphy of the Siberian Sector of the Arctic Ocean and adjacent Laptev Sea Shelf. J. Geophys. Res. Solid Earth 119, 5275–5289. https://doi.org/10.1002/2013JB010727.
West, C.K., Greenwood, D.R., Basinger, J.F., 2015. Was the Arctic Eocene 'rainforest' monsoonal? Estimates of seasonal precipitation from early Eocene megafloras from Ellesmere Island, Nunavut. Earth Planet. Sci. Lett. 427, 18–30. https://doi.org/10.1016/j.epsl.2015.06.036.
Westerhold, T., Marwan, N., Drury, A.J., Liebrand, D., Agnini, C., Anagnostou, E., Barnet, J.S.K., et al., 2020. An astronomically dated record of Earth's climate and its predictability over the last 66 million years. Science 369 (6509), 1383–1387. https://doi.org/10.1126/science.aba6853.